

The 1-acetyl-3-methyl-4-[3-methoxy-4-(4-methylbenzoxy)benzylidene-amino]-4,5-dihydro-1H-1,2,4-triazol-5-one molecule investigated by a joint spectroscopic and quantum chemical calculations



Halil Gökce^a, Onur Akyildirim^b, Semiha Bahçeli^{c,*}, Haydar Yüksek^d, Özlem Gürsoy Kol^d

^a Vocational High School of Health Services, Giresun University, 28200 Giresun, Turkey

^b Department of Chemical Engineering, Faculty of Engineering and Architecture, Kafkas University, 36100 Kars, Turkey

^c Physics Department, Faculty of Arts and Science, Süleyman Demirel University, 32260 Isparta, Turkey

^d Chemistry Department, Faculty of Arts and Science, Kafkas University, 36100 Kars, Turkey

HIGHLIGHTS

- The compounds containing 1,2,4-triazol, their derivatives and synthesis.
- Antioxidant activities of the synthesized compound.
- FT-IR, micro-Raman and UV spectroscopies of the synthesized compound.
- Quantum chemical calculations of the synthesized compound.

ARTICLE INFO

Article history:

Received 2 September 2013

Received in revised form 25 September 2013

Accepted 15 October 2013

Available online 24 October 2013

Keywords:

Antioxidant

1,2,4-Triazole derivatives

Vibrational and UV–Vis spectroscopies

NBO

NLO

DFT method

ABSTRACT

In this study, the synthesis, spectroscopic (FT-IR, micro-Raman and UV–Vis) investigations and antioxidant activity of 1-acetyl-3-methyl-4-[3-methoxy-4-(4-methylbenzoxy)benzylideneamino]-4,5-dihydro-1H-1,2,4-triazol-5-one molecule have been verified. The quantum chemical computations (molecular structure, vibrational frequencies, electronic absorption maximum wavelengths in gas phase and ethanol solvent, HOMO–LUMO, molecular electrostatic potential (MEP) and natural bond orbital (NBO) analyses, nonlinear optical (NLO) and thermodynamic properties and atomic charges of the title compound have been performed using the DFT/B3LYP method with 6-31G(d) basis set. The energetic behavior of title molecule in different solvent media was investigated at the B3LYP/6-31G(d) level by using the integral equation formalism polarizable continuum model (IEFPCM). A comparison between the calculated results and experimental data exhibits a very good agreement.

© 2013 Elsevier B.V. All rights reserved.

1. Introduction

It is well-known that the antioxidants have received a great deal of attention due to their capacities to protect organisms and cells from the damages induced by oxidation stress for the last two decades [1]. In this context, the 1,2,4-triazole ring is a building block of various compounds which possess several biological activities such as antimicrobial, antifungal, anti-inflammatory, antioxidant, antiviral, anticancer, analgesic, and anticonvulsant activity depending on the substituents in the ring system and some *N*-arylideneamino-4,5-dihydro-1H-1,2,4-triazol-5-one derivatives were synthesized [2–8]. Very recently, we have investigated three different antioxidants 3-alkyl-4-[3-methoxy-4-(4-methylbenzoxy)benzylideneamino]-4,5-dihydro-1H-1,2,4-triazol-5-one mole-

cules in terms of spectroscopic and quantum chemical computations by using density functional theory (DFT) combined with the B3LYP/6-31G(d) level [9].

As a continuation of our previous work on antioxidants, in this study we report the synthesis, antioxidant activity and the calculated results of molecular geometry, vibrational spectra, electronic properties, atomic charges and thermodynamic parameters at the B3LYP/6-31G(d) level of 1-acetyl-3-methyl-4-[3-methoxy-4-(4-methylbenzoxy)benzylideneamino]-4,5-dihydro-1H-1,2,4-triazol-5-one molecule as well as the experimental data.

2. Experimental

2.1. Materials and synthesis of the sample

Chemical reagents and all solvents in the study were purchased from Merck AG, Aldrich and Fluka. Melting point which is uncor-

* Corresponding author. Tel.: +90 246 211 40 16.

E-mail address: semihabahceli@sdu.edu.tr (S. Bahçeli).

rected was determined in open glass capillaries by using an Electrothermal digital melting point apparatus.

Scheme 1 shows the synthesis route of 1-acetyl-3-methyl-4-[3-methoxy-4-(4-methylbenzoxy)benzylideneamino]-4,5-dihydro-1H-1,2,4-triazol-5-one (**4**) which was obtained from the reaction of compound (**3**) with acetic anhydride. The starting compound 3-methyl-4-[3-methoxy-4-(4-methylbenzoxy)benzylideneamino]-4,5-dihydro-1H-1,2,4-triazol-5-one (**3**) was prepared according to the literature [9–11].

Meanwhile the preparation of the sample **4** was as follows. The corresponding compound **3** (0.01 mol) was refluxed with acetic anhydride (20 mL) for 0.5 h. After addition of absolute ethanol (100 mL), the mixture was refluxed for 0.5 h. more. Evaporation of the resulting solution at 40–45 °C *in vacuo* and several recrystallizations of the residue from EtOH gave pure compound **4** as colorless crystals.

2.2. Apparatus

UV absorption spectra were measured in 10 mm quartz cells between 200 and 400 nm using a T80 UV/Vis spectrometer PG Instruments Ltd. Extinction coefficients (ϵ) are expressed in $\text{L mol}^{-1} \text{cm}^{-1}$.

IR spectrum of the title compound **4** was recorded at room temperature on a Perkin Elmer Spectrum One FT-IR (Fourier Transform Infrared) Spectrometer with a resolution of 4 cm^{-1} in the transmission mode. The prepared sample were compressed into self-supporting pellet and introduced into an IR cell equipped with KBr window. On the other hand, the micro-Raman (μ -Ra) spectra of the title molecule was recorded by using a Jasco NRS-3100 micro-Raman Spectrophotometer (1800 lines/mm grating and high sensitivity cooled CCD) at room temperature in the region $50\text{--}4000 \text{ cm}^{-1}$. The micro-Raman spectrometer was calibrated with the silicon phonon mode at 520 cm^{-1} and microscope objective 100x was used. The 632.8 nm lines of He-Ne laser was used for excitation. The exposure time was taken as 10 s for each sample and 50 scans were accumulated.

2.3. Antioxidant activity tests

The antioxidant properties of newly synthesized compound **4** and standard antioxidants butylated hydroxytoluene (BHT), butyl-

ated hydroxyanisole (BHA) and α -tocopherol were studied and evaluated using different antioxidant tests; including reducing power, free radical scavenging and metal chelating activity.

The reducing power of the synthesized compounds and standards was determined according to the method of Oyaizu [12]. The reductive capability of compound is assessed by the extent of conversion of the Fe^{3+} /ferricyanide complex to the Fe^{2+} /ferrous form. High absorbance at 700 nm indicates high reducing power.

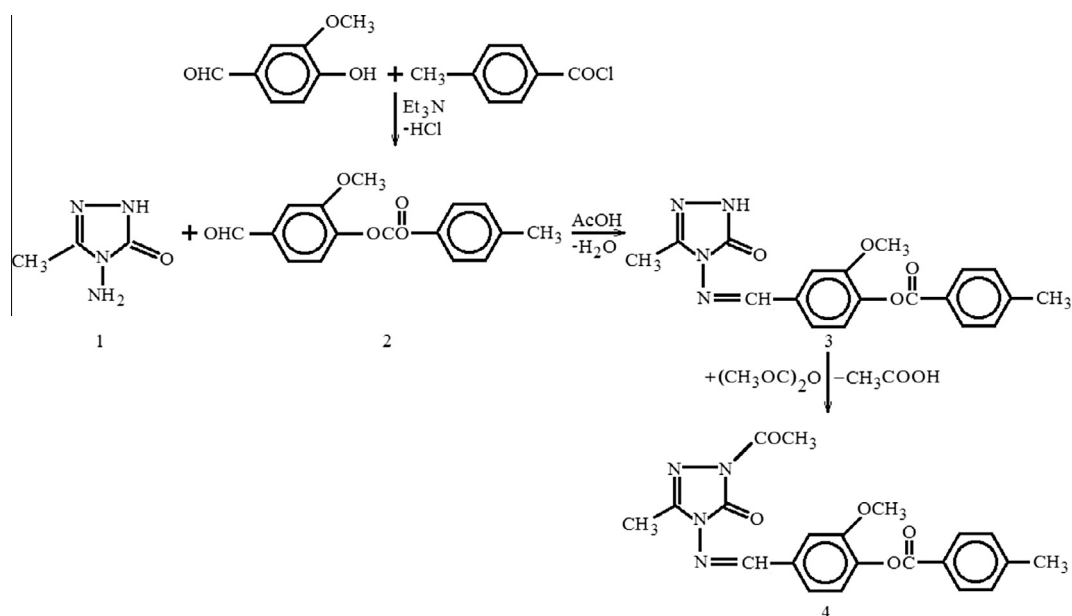
Free radical scavenging activity of the synthesized compounds and standards was measured via DPPH (2,2-diphenyl-1-picrylhydrazyl) by using the method of Blois [13]. The reduction capability of DPPH radicals was determined by decrease in its absorbance at 517 nm induced by antioxidants. The absorption maximum of a stable DPPH radical in ethanol was at 517 nm. The decrease in absorbance of DPPH radical was caused by antioxidants for the reaction between antioxidant molecules and radical, progresses, which result in the scavenging of the radical by hydrogen donation. It is visually noticeable as a discoloration from purple to yellow. Hence, DPPH is usually used as a substrate to evaluate antioxidative activity of antioxidants [14].

The chelation of ferrous ions by the synthesized compounds and standards was estimated by the method of Dinis et al. [15]. Ferrous ion can quantitatively form complexes with Fe^{2+} . In the presence of chelating agents, the complex formation is disrupted with the result that the red color of the complex is decreased. Measurement of color reduction, in its absorbance at 517 nm, therefore allows estimation of the chelating activity of the coexisting chelator [16].

3. Computational details

The optimized molecular structure, vibrational frequencies, UV-Vis spectroscopic parameters, NBO analysis, NLO properties, thermodynamic parameters, atomic charges and frontier molecule orbitals (HOMO – 1, HOMO, LUMO, LUMO + 1) of the compound **4** have been calculated by using DFT/B3LYP method with 6-31G(d) basis set. All quantum chemical calculations were carried out by using Gaussian 03 program package and the GaussView molecular visualization program [17,18].

The molecular structure and vibrational calculations of the compound **4** was computed by using Becke-3-Lee Yang Parr



Scheme 1. Syntheses route of compound **4**.

(B3LYP) [19,20] density functional method with 6-31G(d) basis set in ground state. The positive values of all calculated vibrational wavenumbers indicate the stability of the optimized molecular structures and since the computed wavenumber values at these levels contain the well-known systematic errors, the calculated vibrational wavenumbers were scaled with 0.9614 ranges from 1700 to 4000 cm^{-1} and were scaled with 1.0013 lower than 1700 cm^{-1} for B3LYP/6-31G(d) level [21,22]. Meanwhile the assignments of fundamental vibrational modes of the title molecule were performed on the basis of total energy distribution (TED) analysis by using VEDA 4 program [23].

As for the UV–Vis calculations of the mentioned molecule we performed them using TD-DFT/B3LYP method in gas phase and ethanol solvent [24]. In addition, the HOMO – 1, HOMO, LUMO and LUMO + 1 energy values and energy gaps of compound **4** were calculated at the B3LYP/6-31G(d) level. Likewise the orbital shapes (HOMO – 1, HOMO, LUMO and LUMO + 1) of the mentioned molecule in 3-dimension were plotted at the same level. The plot of molecular electrostatic potential (MEP) map of title molecule was verified in 3-dimension using the optimized molecular structure at B3LYP/6-31G(d) level. Furthermore, the energetic behavior in different solvent media, thermodynamic properties and Mulliken and NBO atomic charges of title molecule were calculated at the mentioned level.

The Raman activities (S_i) calculated by using Gaussian 03 program have been converted to relative Raman intensities (I_i) using the following relationship

$$I_i = \frac{f(v_0 - v_i)^4 S_i}{v_i [1 - \exp(-hc v_i / kT)]},$$

where v_0 (cm^{-1}) is the exciting units, v_i is the vibrational wavenumber of the i th normal mode, h , c , and k are well-known universal constants and f is the suitably chosen common scaling factor for all the peak intensities [25,26].

4. Results and discussion

4.1. Molecular geometry

The optimized molecular structure at the B3LYP/6-31G(d) level of 1-acetyl-3-methyl-4-[3-methoxy-4-(4-methylbenzoyl)benzylideneamino]-4,5-dihydro-1H-1,2,4-triazol-5-one molecule is shown in Fig. 1. The calculated molecular geometric parameters at the B3LYP/6-31G(d) level are listed in Table S1 (Supplementary materials). The calculated double N3=C2 and N7=C8 bond lengths were found as 1.295 Å and 1.291 Å, while the single N1=C2, N1=C5 and N4=C5 bond lengths in 1,2,4-triazol ring are calculated as 1.390, 1.406 and 1.399 Å, respectively. Likewise the calculated double C5=O6 bond length in 1,2,4-triazol ring and the C18=O19 and C28=O50 bond lengths in aliphatic ketone groups were found as 1.222, 1.204 and 1.208 Å, respectively. The difference between the calculated C=O bond lengths in aromatic and aliphatic groups arised from the reasons such as the charge density of oxygen atom bounded to the ring and the size of ring. The calculated single C12=O15 and O15=C16 bond lengths were found as 1.359 and 1.421 Å, respectively, due to the fact that the electron density are more localized on methyl groups. The C–C bond lengths in phenyl rings of title molecule are calculated at the interval 1.389–1.417 Å. By considering Table S1 (Supplementary materials), the calculated C2=C27, C8=C9, C18=C20, C25=C26 and C28=C46 bond lengths were found as 1.487, 1.462, 1.489, 1.510 and 1.510 Å, respectively, which are longer than the other C–C bond lengths.

On the other hand, the potential energy surface (PES) scan of the title molecule was performed by changing of torsion angle at 10° steps from 0° to 360° around the C8–C9 bond axis of the

N7–C8–C9–C10 dihedral angle which is positioned between the 1,2,4-triazol and phenyl rings as shown in Fig. 1 and was calculated as 0.527° with B3LYP method at 6-31G(d) basis set. The shape of PES for 1-acetyl-3-methyl-4-[3-methoxy-4-(4-methylbenzoyl)benzylideneamino]-4,5-dihydro-1H-1,2,4-triazol-5-one molecule as a function of N7–C8–C9–C10 dihedral angle is given in Fig. 2. Therefore, there are three possible conformation states of the title molecule. The energy value of C1 conformation shows a minimum energy value of –1407.3857 Hartrees calculated at the B3LYP/6-31G(d) level and becomes the most stable state of 1-acetyl-3-methyl-4-[3-methoxy-4-(4-methylbenzoyl)benzylideneamino]-4,5-dihydro-1H-1,2,4-triazol-5-one molecule. Furthermore, the C3 conformer becomes the second stable conformation with an energy value of –1407.3849 Hartrees. However, the C2 conformation is the most unstable state of title molecule due to the energy value of –1407.3724 Hartrees at the mentioned level.

4.2. Vibrational frequencies

The 1-acetyl-3-methyl-4-[3-methoxy-4-(4-methylbenzoyl)benzylideneamino]-4,5-dihydro-1H-1,2,4-triazol-5-one molecule have 50 atoms and the number of the normal vibrations is 143. All vibrations of molecules under C_1 symmetry are active in both IR and Raman. The observed and calculated vibrational frequencies, the calculated IR intensities and Raman scattering activities and assignments of vibrational frequencies for compound **4** are summarized in Table 2. Furthermore the experimental and simulated at B3LYP/6-31G(d) level IR and micro-Raman spectra of the compound **4** are given in Figs. 3 and 4, respectively. The frequency values for C2 vs C3 conformers were verified and two imaginary frequency values for C2 conformer was found. This indicates that the C2 conformer is an unstable transition state. However there is no imaginary vibrational frequency value for the C3 conformer and on the contrary the calculated vibrational frequency values for this conformation are very close to those of stable state C1 conformer.

4.2.1. CH vibrations

The C–H stretching bands of aromatic ring can be assigned to the observed bands at 3013 (IR)–3015 (R), 3033 (IR)–3034 (R) and 3080 (IR)–3078 (R) cm^{-1} for the compound **4** since the C–H stretching vibrations of aromatic compounds are arised above 3000–3100 cm^{-1} [27–32]. Likewise the observed bands at 1463 (IR), 1347 (IR)–1347 (R), 1311 (IR)–1309 (R), 1258 (IR)–1260 (R), 1212 (R) and 1153 (IR)–1148 (R) cm^{-1} of the title molecule can be attributed to the C–H in-plane bending vibrations combined with other vibration bands, while the observed bands at 976 (IR)–982 (R), 963 (IR)–964 (R), 862 (IR)–872 (R), 833 (IR)–837 (R), 820 (IR)–823 (R) and 782 (IR)–785 (R) cm^{-1} can be assigned to the C–H out-of-plane bending vibrations [27–29]. The calculated wavenumber values and assignments for the C–H stretching, in-plane and out-of-plane bending modes are given in Table 2.

On the other hand for the aliphatic=C–H group the C–H stretching vibration bands are observed at 3056 (IR)–3058 (R) cm^{-1} as weak bands and the calculated C–H stretching vibration band value at the B3LYP/6-31G(d) level was found as 3069.20 cm^{-1} . Furthermore aliphatic CH in-plane vibration of the title molecule can be assigned to the observed strong band at 1385 (IR) cm^{-1} while the observed strong band at 1015 (IR) cm^{-1} can be attributed to the CH out-of-plane bending vibration mode of aliphatic group [27].

4.2.2. CH₃ vibrations

The observed weak band at 2977 cm^{-1} in IR spectrum of title molecule can be attributed to the CH₃ symmetric stretching mode,

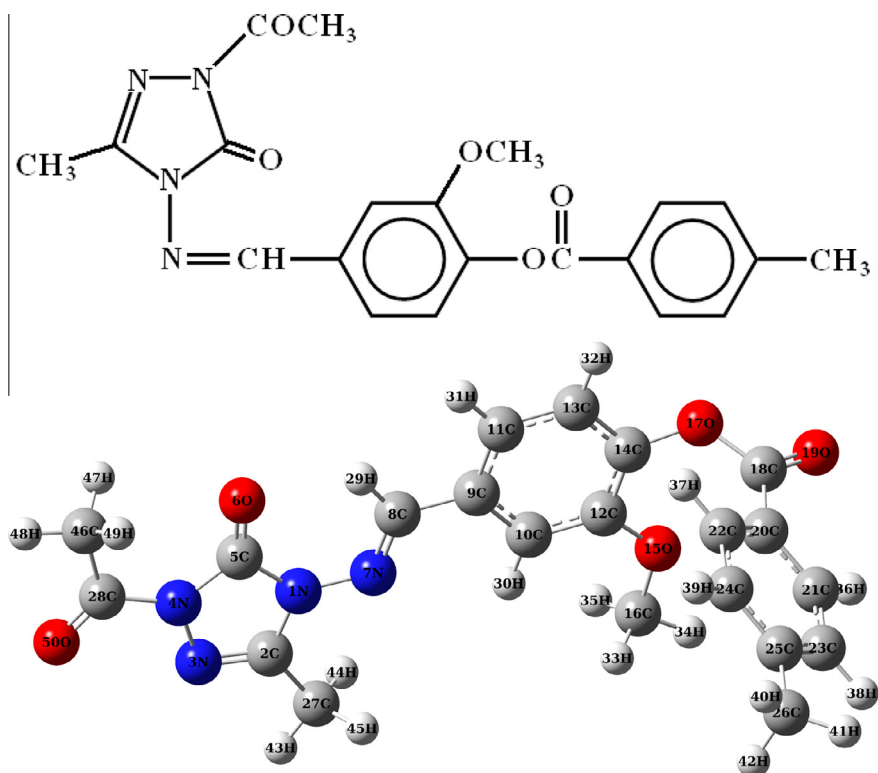


Fig. 1. The chemical structure (top) and optimized molecular structure (bottom) of 1-acetyl-3-methyl-4-[3-methoxy-4-(4-methylbenzyloxy)benzylideneamino]-4,5-dihydro-1H-1,2,4-triazol-5-one molecule (**4**) with DFT/B3LYP/6-31G(d) level.

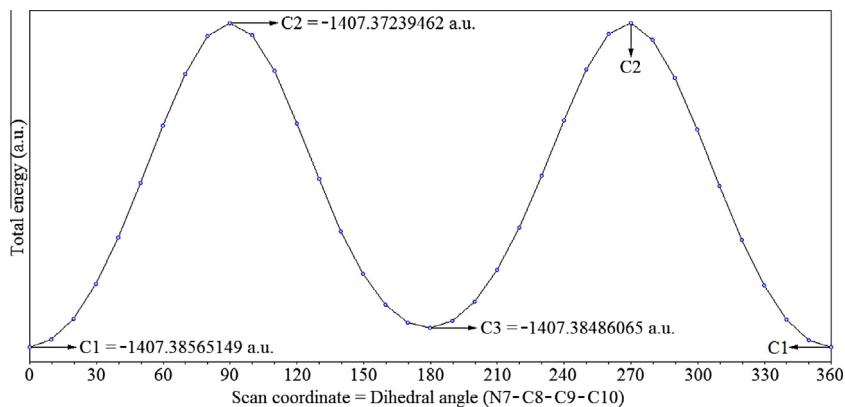


Fig. 2. The scanned potential energy surface with DFT/B3LYP/6-31G(d) level of 1-acetyl-3-methyl-4-[3-methoxy-4-(4-methylbenzyloxy)benzylideneamino]-4,5-dihydro-1H-1,2,4-triazol-5-one molecule (**4**).

while the observed weak bands at 2917 (IR)–2917 (R) and 2944 (IR)–2947 (R) cm^{-1} can be assigned to the CH_3 asymmetric stretching mode. Likewise, the observed bands at 1509 (IR)–1507 (R), 1500 (IR) and 1487 (IR) cm^{-1} can be attributed to the scissoring modes of CH_3 groups of the compound **4**. On the other hand, the symmetric bending bands of CH_3 groups are observed at 1463 (IR) and 1414 (IR)–1414 (R) cm^{-1} . Similarly, the rocking bands of CH_3 groups are observed at 1177 (IR), 1153 (IR)–1148 (R) and 1071 (IR)–1070 (R) cm^{-1} for the compound **4**. On the other hand it is well-known that the torsion modes of methyl groups arise below 400 cm^{-1} for organic compounds [27–32]. Although this band was not observed for our molecule, the computed values for the torsion bands of methyl groups were found as 168.38, 170.04 and 263.98 cm^{-1} . We can easily state that the vibrational wavenumbers for methyl groups of the mentioned molecule given in Table 2 are in good agreement with experimental data.

On the other hand the calculated intensities of observed bands around the 3000 cm^{-1} region with weak intensities associated with stretching of C–H, =C–H and CH_3 were found as almost the same.

4.2.3. CC, CN and NN vibrations

For the compound **4** the observed peaks are at 1631 (IR)–1628 (R), 1611 (IR)–1608 (R), 1463 (IR) and 1373 (IR)–1378 (R) cm^{-1} can be assigned to the CC vibrational stretching bands of aromatic rings. The CCC in-plane bending modes of aromatic rings can be attributed to the observed bands at 1028 (IR/R), 794 (IR), 570 (IR)–568 (R) and 536 (IR)–537 (R) cm^{-1} . Likewise, the CCC torsion modes of aromatic ring in compound **4** are observed at 468 (IR), 429 (IR/R) and 415 (IR)–412 (R) cm^{-1} .

The C=N stretching vibrations of 1,2,4-triazol ring were observed at 1693 (IR)–1697 (R) cm^{-1} while the calculated value of

Table 2

The observed IR, Raman frequencies, calculated frequencies, relative intensities and probable assignments of 1-acetyl-3-methyl-4-[3-methoxy-4-(4-methylbenzyloxy)benzylidenedamino]-4,5-dihydro-1*H*-1,2,4-triazol-5-one molecule (**4**).

Assignments (TED% > 10%)	Experimental (cm ⁻¹)		The calculated with B3LYP/6-31G(d) level					
	IR	Raman	For C1 conformer				For C2 conformer	For C3 conformer
			Unscaled freq.	Scaled freq.	I _{IR}	S _{Raman}	Scaled freq.	Scaled freq.
Lattice mode	–	–	11.67	11.68	0.267	2.894	–99.03	12.12
Lattice mode	–	–	15.31	15.33	0.797	5.241	–11.07	13.61
Lattice mode	–	–	31.40	31.44	0.458	7.369	14.55	16.74
Lattice mode	–	–	35.57	35.62	0.848	1.776	16.74	32.60
Lattice mode	–	–	39.64	39.69	0.545	1.850	28.61	32.98
Lattice mode	–	–	50.75	50.82	0.615	3.695	38.70	38.43
Lattice mode	–	–	53.39	53.46	0.245	0.574	42.86	50.13
Lattice mode	–	–	65.57	65.65	3.146	0.969	52.38	65.76
Lattice mode	–	–	77.88	77.98	2.596	0.635	69.79	77.59
Lattice mode	–	–	85.17	85.28	7.481	1.563	76.58	86.16
Lattice mode	–	–	93.70	93.82	2.941	1.264	91.45	91.89
–	–	107 s	109.40	109.54	0.785	1.129	97.00	109.16
γCCNN(12)	–	–	122.61	122.77	0.817	2.165	105.13	130.08
γCCNN(16)	–	–	133.71	133.88	0.291	1.711	130.43	137.56
δCCC(13) + τNNCC(12) + γCNCC(12)	–	151 sh	155.39	155.60	0.238	3.263	136.92	149.60
τCH ₃ (59)	–	–	168.17	168.39	0.383	0.264	149.34	161.27
τCH ₃ (45) + γCCNN(11)	–	–	169.82	170.04	0.323	0.297	161.99	161.76
δCCC(18) + τCNCC(12)	–	–	176.24	176.47	0.369	1.362	163.30	166.25
τCNCC(17) + τNCCC(14)	–	190 w	188.34	188.58	1.808	0.744	177.44	174.58
δCCN(18) + δCNC(17)	–	–	202.46	202.72	9.954	1.931	196.76	191.22
δCNC(12)	–	–	210.44	210.71	3.454	1.074	199.13	216.65
τNCCC(13)	–	–	220.62	220.91	6.090	0.377	216.11	225.51
–	–	241 w	237.06	237.37	11.371	0.593	242.93	245.17
τCH ₃ (36) + γCCCC(12) + τNCNN(11)	–	–	263.64	263.98	1.161	0.589	254.43	270.09
γCCCC(32)	–	290 w	279.72	280.08	3.505	4.982	280.63	279.84
δCCO(15) + δCCN(14)	–	–	304.02	304.42	3.558	2.896	299.86	303.40
τNCNN(19)	–	–	320.14	320.56	3.475	4.547	311.78	316.34
–	–	–	341.47	341.91	2.715	1.825	330.78	340.50
δCCC(19)	–	–	351.28	351.73	2.500	3.222	350.58	348.80
δCCC(42)	–	351 m	352.58	353.04	4.722	0.341	361.10	353.71
γCNCC(29) + τCNCC(19)	–	–	362.33	362.80	5.389	0.579	362.07	363.34
δOCN(31) + δCCN(27)	–	–	378.04	378.54	2.274	2.092	375.84	378.63
δCOC(15)	–	–	402.90	403.43	2.343	3.330	411.60	401.79
τCCCC(34) + τCCCO(11) + τHCCC(10)	415 m	412 w	418.67	419.22	0.075	0.227	418.19	417.23
τCCCC(15)	429 w	429 w	428.44	429.00	1.782	5.193	425.10	421.62
δNCC(14)	449 w	–	448.28	448.86	33.374	2.800	443.50	436.71
τCCCC(14)	468 m	–	466.88	467.49	1.552	0.486	463.90	467.23
γCCCC(13)	–	474 w	476.61	477.23	1.912	7.845	477.14	479.41
τCCCC(13) + γCCCC(13) + γOCCC(12)	–	–	491.20	491.84	3.169	10.201	496.64	495.23
δCOC(10)	536 m	537 w	533.48	534.18	4.793	3.912	536.13	532.98
δCOC(19) + δCCC(11)	570 m	568 w	570.76	571.50	8.001	5.690	574.20	574.89
γONNC(60) + ρCH ₃ (16)	–	–	582.55	583.31	3.666	1.118	583.02	583.40
δCOC(20) + δCCO(16) + δCCC(12)	–	–	595.30	596.07	4.190	2.828	589.75	591.64
δOCO(17)	–	–	601.24	602.02	14.862	2.945	598.52	604.91
δOCC(29) + νC–CH ₃ (27)	609 s	–	612.69	613.48	75.911	10.667	603.56	613.17
γOCCC(19) + τHCCC(14)	637 m	641 m	633.19	634.01	12.364	4.827	613.08	631.24
–	–	–	639.77	640.60	13.500	4.600	650.85	648.46
τNNCC(28) + δCCC(26)	651 sh	647 w	652.60	653.45	2.072	7.195	654.11	653.52
δCCC(36) + τNNCC(13)	–	–	654.81	655.66	1.472	2.121	654.89	655.53
δCNC(17) + δCCN(14) + δOCN(14) + νC–CH ₃ (11)	675 m	–	673.55	674.42	15.698	6.968	676.04	677.73
γOCOC(18)	682 w	–	696.22	697.13	18.707	5.199	699.55	692.73
–	–	–	709.15	710.07	10.600	9.008	706.13	707.19
γONNC(57)	729 m	717 w	718.37	719.31	16.082	3.344	724.38	719.13
γOCCC(24) + τCCCO(14)	740 s	746 w	720.88	721.82	1.293	3.140	725.60	721.99
δCCC(11)	–	–	760.88	761.87	76.849	7.212	761.32	764.88
γOCOC(26) + τHCCC(25)	782 m	785 s	764.65	765.64	31.414	4.875	766.19	769.73
δCCC(14) + νC–CH ₃ (12) + νCC(11)	794 w	–	807.64	808.69	8.281	18.368	806.45	817.92
τHCCC(58)	820 w	823 w	818.91	819.98	3.481	22.376	821.15	827.48
τHCCC(52)	833 m	837 w	836.25	837.33	15.942	6.436	842.38	846.36
τHCCC(84)	–	–	850.37	851.48	18.813	1.832	851.99	852.47
τHCCC(70)	862 m	–	860.36	861.48	3.294	3.507	861.12	862.54
δOCO(12)	878 s	880 m	885.28	886.43	5.440	4.522	869.58	866.54
τHCCC(69)	–	–	889.28	890.44	19.336	1.246	884.20	883.93
νC–CH ₃ (17) + νNC(12)	–	–	920.42	921.62	18.997	10.490	921.88	927.52
τHCCC(76)	–	–	940.87	942.09	1.997	2.127	944.24	961.65
τHCCC(81)	963 w	964 w	969.54	970.81	3.163	1.656	969.22	968.76
τHCCC(70)	976 m	982 w	982.23	983.50	1.522	2.279	974.90	971.67
ρCH ₃ (26) + νC–CH ₃ (16)	–	–	982.86	984.14	33.726	10.924	983.16	985.01
νCC(20) + νO–CH ₃ (10)	–	–	997.59	998.88	2.625	4.576	984.64	985.76
τHCNN(82)	1015 s	–	1017.54	1018.87	7.456	11.616	996.69	1017.33

(continued on next page)

Table 2 (continued)

Assignments (TED% > 10%)	Experimental (cm ⁻¹)		The calculated with B3LYP/6-31G(d) level					
	IR	Raman	For C1 conformer				For C2 conformer	For C3 conformer
			Unscaled freq.	Scaled freq.	I _{IR}	S _{Raman}	Scaled freq.	Scaled freq.
ρCH ₃ (43)	–	–	1018.03	1019.35	46.519	2.826	1018.91	1019.69
δCCC(35)	1028 m	1028 w	1032.98	1034.32	173.740	8.014	1036.09	1034.54
ρCH ₃ (52)	–	–	1037.74	1039.09	71.017	7.381	1039.63	1039.76
νOC(30) + νCC(15)	1054 vs	–	1062.27	1063.65	258.997	13.403	1069.88	1064.76
ρCH ₃ (65)	–	–	1070.67	1072.07	6.913	0.762	1071.90	1072.10
νO–CH ₃ (59)	–	–	1072.57	1073.96	39.638	5.592	1075.92	1073.86
ρCH ₃ (73)	1071 m	1070 w	1075.52	1076.92	9.267	0.305	1076.16	1075.94
ρCH ₃ (97)	–	–	1081.34	1082.75	2.635	0.778	1081.74	1082.42
δNNC(13) + νNC(10)	–	–	1096.58	1098.01	83.032	15.268	1099.59	1098.78
νNN(25) + ρCH ₃ (16)	1123 s	–	1150.79	1152.29	0.399	28.239	1150.23	1151.45
δHCC(54)	1153 s	1148 s	1153.34	1154.84	4.264	3.960	1154.76	1155.60
δHCC(43)	–	–	1158.25	1159.76	96.404	100.644	1158.43	1156.39
ρCH ₃ (98)	1177 s	–	1185.56	1187.10	1.400	4.333	1186.14	1186.10
νOC(15) + νCC(11) + ρCH ₃ (11)	1201 vs	1193 s	1198.86	1200.42	126.029	370.022	1200.29	1205.05
δHCC(29)	–	1212 w	1213.33	1214.91	252.851	67.498	1214.39	1215.53
δHCC(35)	–	–	1217.20	1218.78	31.122	25.509	1219.03	1220.43
ρCH ₃ (35) + νCC(11)	–	–	1231.48	1233.08	17.424	216.201	1228.77	1232.54
νCC(35)	–	–	1240.38	1241.99	48.611	26.444	1242.00	1242.08
νOC(23) + δHCC(16)	1258 vs	1260 vs	1248.87	1250.49	231.287	42.717	1251.78	1252.63
νCC(27) + νOC(10)	1276 w	–	1270.49	1272.14	146.309	58.012	1272.28	1272.11
δNCN(20) + νNN(13)	–	–	1286.32	1287.99	48.423	192.490	1283.66	1292.03
δHCC(54) + νCC(11)	1311 vs	1309 w	1305.75	1307.44	198.419	153.928	1306.86	1308.81
νOC(16) + δHCC(10)	–	–	1323.95	1325.67	543.024	174.745	1329.67	1332.63
νNC(45) + δNCN(10)	–	–	1331.05	1332.78	446.952	115.914	1331.87	1337.76
δHCC(71) + νCC(13)	1347 m	1347 w	1348.64	1350.40	0.679	0.931	1350.66	1351.92
νCC(53)	–	–	1355.31	1357.07	1.001	3.500	1351.80	1357.16
νCC(46)	1374 m	1378 w	1363.70	1365.47	2.038	7.794	1356.70	1366.32
δHCN(25) + νNC(23) + δCH ₃ (12)	1385 s	–	1397.11	1398.93	123.999	13.329	1384.84	1394.96
δCH ₃ (76)	1414 s	1414 m	1429.89	1431.75	35.555	6.470	1430.95	1431.79
δCH ₃ (83) + δHCN(11)	–	–	1442.98	1444.86	17.633	28.721	1437.38	1439.32
δCH ₃ (74) + δHCN(11)	–	–	1443.05	1444.93	16.514	29.448	1443.70	1445.32
δHCC(41)	1450 w	1454 m	1453.37	1455.25	8.863	4.099	1451.46	1454.78
νCC(35) + δCH ₃ (19)	1463 m	–	1465.83	1467.73	56.946	257.626	1455.16	1455.74
νNC(25) + δHCN(19) + δ _s CH ₃ (10)	–	–	1468.25	1470.16	222.746	2.612	1464.15	1474.66
δ _s CH ₃ (98)	1487 w	–	1480.46	1482.39	21.361	9.398	1481.91	1482.35
δ _s CH ₃ (98)	1500 s	–	1500.75	1502.70	10.163	16.928	1501.56	1502.56
δ _s CH ₃ (100)	–	–	1501.96	1503.91	8.182	23.083	1503.06	1503.32
δ _s CH ₃ (62)	1509 w	1507 w	1508.22	1510.18	1.264	129.733	1507.28	1508.45
δ _s CH ₃ (58)	–	–	1511.94	1513.90	9.291	29.896	1510.94	1513.58
δ _s CH ₃ (81)	–	–	1517.12	1519.09	7.201	18.494	1517.70	1518.15
δ _s CH ₃ (71)	–	–	1520.62	1522.60	8.898	5.805	1521.92	1522.41
δ _s CH ₃ (88)	–	–	1520.78	1522.76	9.635	32.987	1522.24	1523.54
δ _s CH ₃ (92)	–	–	1531.17	1533.16	60.564	8.778	1533.23	1533.69
δHCC(32)	–	–	1553.17	1555.19	146.042	75.966	1559.12	1560.44
δHCC(58)	1581 m	1592 vs	1559.29	1561.32	4.621	2.436	1561.96	1563.62
νCC(59)	1611 s	1608 sh	1625.31	1627.43	3.585	3.898	1627.27	1625.36
νCC(21)	1631 s	1628 sh	1627.92	1630.03	23.133	217.320	1635.39	1627.81
νCC(33) + δHCC(16)	–	–	1646.72	1648.86	61.567	3447.716	1659.04	1654.69
νCC(22) + δHCC(21)	–	–	1669.44	1671.61	48.123	122.331	1671.88	1671.34
νNC(50) + νCC(13)	–	–	1670.99	1673.16	29.320	613.742	1675.86	1672.72
νNC(62)	1693 s	1697 w	1685.33	1687.53	142.470	587.812	1696.06	1688.30
νOC(78)	1744 vs	1740 s	1802.03	1732.47	275.223	7.107	1734.47	1730.59
νOC(88)	1766 s	–	1841.07	1770.01	539.112	31.046	1767.74	1769.59
νOC(76)	1782 w	–	1842.55	1771.42	200.719	112.947	1771.30	1770.65
ν _s CH ₃ (100)	2917 w	2917 vw	3035.97	2918.78	34.692	79.457	2916.92	2917.70
ν _s CH ₃ (96)	–	–	3043.95	2926.45	22.874	207.275	2925.69	2926.41
ν _s CH ₃ (92)	2944 w	2947 w	3069.41	2950.93	7.770	145.099	2952.67	2951.96
ν _s CH ₃ (94)	–	–	3080.69	2961.77	0.471	128.375	2961.48	2961.44
ν _{as} CH ₃ (99)	2977 w	–	3099.25	2979.62	33.709	32.548	2977.63	2978.31
ν _{as} CH ₃ (98)	–	–	3101.36	2981.65	18.532	96.228	2980.57	2981.44
ν _{as} CH ₃ (100)	–	–	3127.40	3006.69	6.218	56.895	3008.26	3007.84
ν _{as} CH ₃ (97)	–	–	3130.31	3009.48	13.390	68.058	3008.78	3009.48
ν _{as} CH ₃ (99)	–	–	3145.82	3024.39	2.284	33.639	3024.32	3024.07
ν _{as} CH ₃ (100)	–	–	3170.60	3048.22	16.405	93.038	3047.74	3048.37
ν _{as} CH ₃ (92)	–	–	3172.33	3049.88	5.540	90.654	3050.55	3050.30
ν _{as} CH ₃ (94)	–	–	3182.44	3059.60	13.214	129.190	3051.38	3059.29
νCH(99)	3013 w	3015 vw	3184.36	3061.45	16.263	106.157	3059.64	3061.57
νCH(99)	3033 w	3034 vw	3187.33	3064.30	12.296	62.581	3060.85	3065.11
νCH(100)	3056 w	3058 vw	3192.42	3069.20	1.449	8.096	3063.72	3066.70

vCH(100)	3080 w	3078 vw	3200.05	3076.52	5.660	66.818	3080.98	3087.85
vCH(84)	-	-	3220.20	3095.90	6.164	162.825	3095.41	3096.24
vCH(100)	-	-	3223.70	3099.26	3.823	84.947	3099.42	3100.49
vCH(99)	-	-	3231.01	3106.29	5.261	74.838	3102.52	3109.21
vCH(99)	-	-	3245.14	3119.88	3.097	24.426	3107.48	3110.32

v, stretching; δ , bending; δ_s , scissoring; ρ , rocking; γ , out-of-plane bending; τ , torsion; s, strong; m, medium; w, weak; v, very; sh, shoulder. IR intensities (km/mole); S_R , Raman scattering activities ($\text{Å}^4/\text{amu}$).

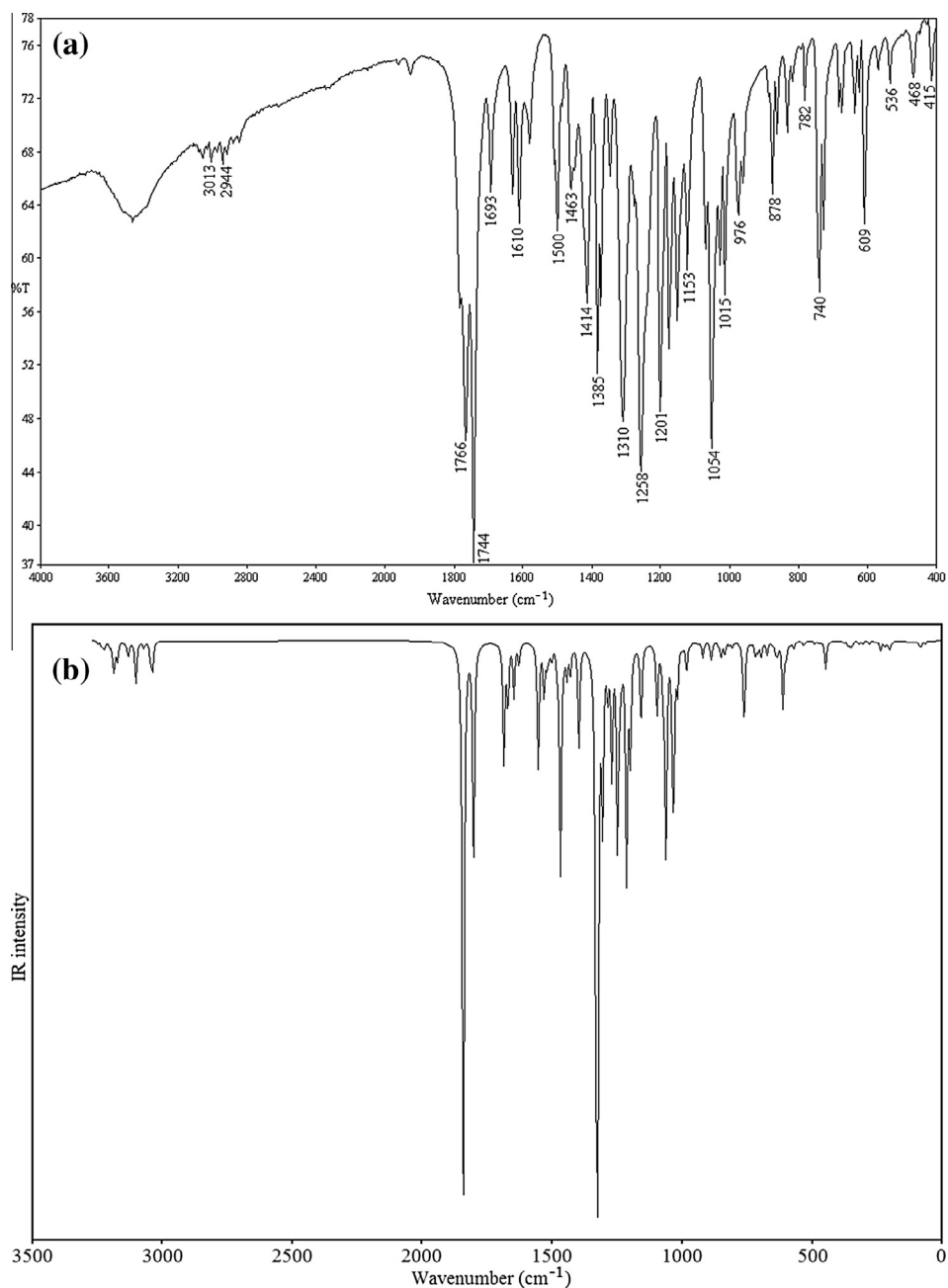


Fig. 3. IR spectra (a) experimental and (b) simulated at the B3LYP/6-31G(d) level of 1-acetyl-3-methyl-4-[3-methoxy-4-(4-methylbenzoxy)benzylideneamino]-4,5-dihydro-1H-1,2,4-triazol-5-one molecule (**4**).

this band was found as 1687.53 cm^{-1} for compound **4**. However for aliphatic group although this band was not observed, the calculated value of the C=N stretching vibration wavenumber of aliphatic group was found as 1673.16 cm^{-1} for the title molecule. Similarly, the NC stretching mode in the compound **4** was observed at $1385 \text{ (IR) cm}^{-1}$ combined with the other vibrational bands. The

calculated values for the NC stretching modes were found as 1398.93 , 1332.78 and 1098.01 cm^{-1} .

The observed strong band at 1123 cm^{-1} in the IR spectrum of title compound can be assigned to the NN stretching mode and the calculated wavenumber values of the mentioned mode were found as 1287.99 and 1152.29 cm^{-1} .

4.2.4. CO vibrations

Since the position of C=O stretching band stretching in the region 1870–1540 cm^{-1} region depends on properties such as the physical state, electronic and mass effects of neighboring substituents, intramolecular and intermolecular hydrogen bonding and conjugations, the C=O vibration band in ester and acetyl groups of compound **4** can be assigned to the band observed at 1782 (IR) cm^{-1} and the observed strong band at 1766 (IR) cm^{-1} , respectively [27–32]. Similarly, the observed bands at 1744 (IR)–1740 (R) cm^{-1} can be attributed to the C=O stretching mode in triazol ring.

The calculated C=O stretching modes in ester, acetyl and triazol groups of title molecule at the B3LYP/6-31G(d) level were found as 1771.42, 1770.01 and 1732.47 cm^{-1} , respectively.

The C(in phenyl ring)–OCH₃ and C14 (in phenyl ring)–O17(in ester) stretching bands combined with other vibrations of the title molecule are observed at 1201 (IR)–1193 (R) cm^{-1} and 1258 (IR)–1260 (R) and 1276 (IR) cm^{-1} , respectively. Their calculated wave-number values were found as 1325.67 and 1200.42 cm^{-1} and 1250.49 cm^{-1} , respectively. Furthermore, the C18–O17 stretching mode in ester group are observed at 1054 cm^{-1} in IR spectrum.

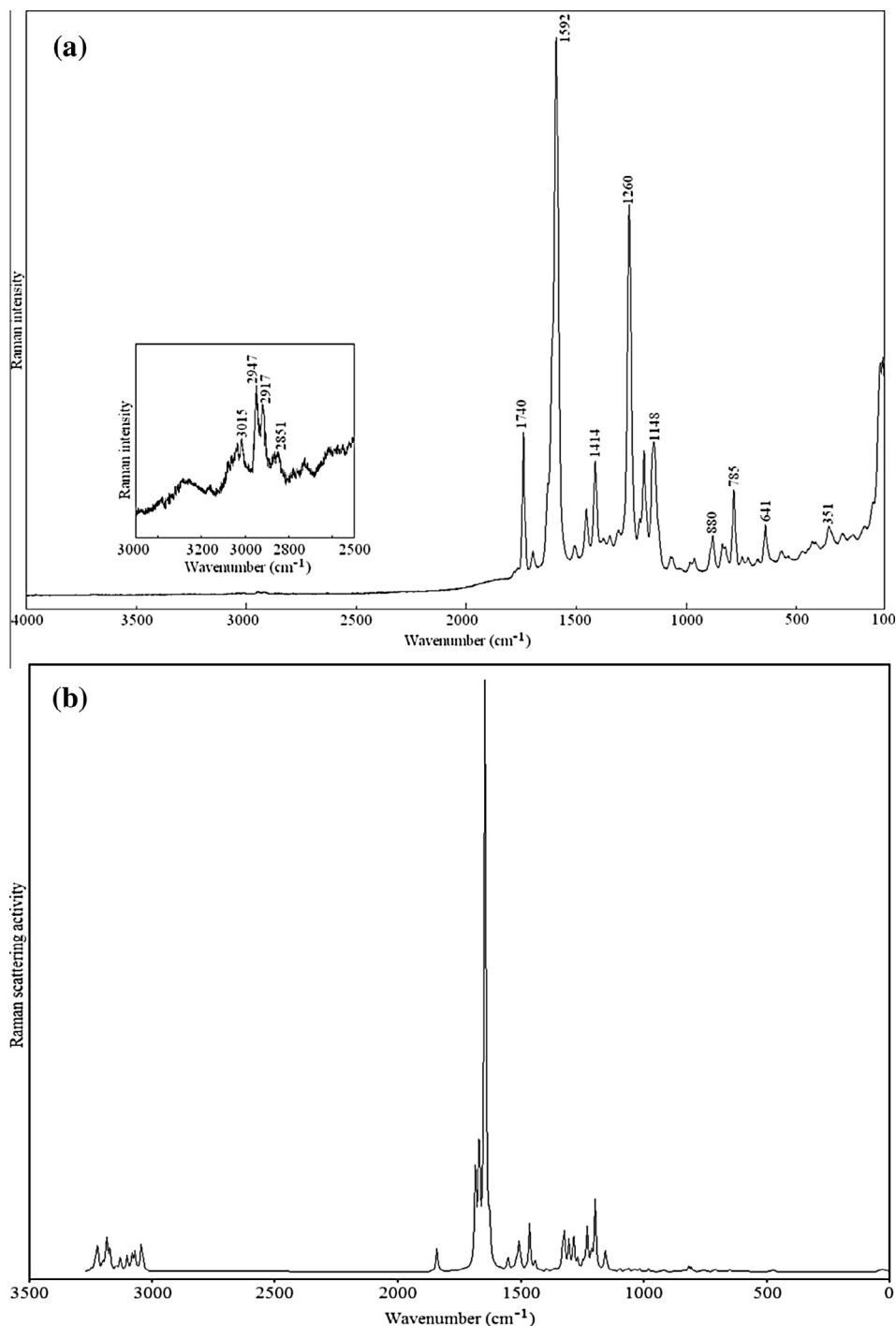


Fig. 4. Raman spectra (a) experimental and (b) simulated at the B3LYP/6-31G(d) level of 3-methyl-4-[3-methoxy-4-(4-methylbenzoxy)benzylideneamino]-4,5-dihydro-1H-1,2,4-triazol-5-one molecule (**4**).

The O—CH₃ stretching vibrations of title molecule are not observed in both IR spectrum and micro-Raman one. However, the calculated value for this mode was found as 1073.96 cm⁻¹.

Likewise, the OCO bending vibration of ester group and COCH₃ bending mode can be attributed to the peaks observed at 878 (IR)–880 (R) cm⁻¹ and 570 (IR)–568 (R) and 536 (IR)–537 (R) cm⁻¹, respectively, as seen in Table 2.

4.3. Electronic absorption and HOMO–LUMO analysis

The experimental electronic absorption maximum wavelengths of the compound **4** in ethanol solvent have been observed at 310, 296 and 242 nm which correspond to the transitions n → π*, π → π* and n → σ*, respectively. The excitation energies, oscillator strengths (*f*) and absorption wavelengths (*λ*) of UV–Vis electron absorption spectroscopy of the title molecule have been calculated in gas phase and ethanol solvent by using TD-DFT/B3LYP method with 6-31G(d) basis set and are presented in Table 3. The calculated electron absorption wavelengths for the compound **4** were found as 321.40, 298.05 and 292.49 nm in gas phase and 324.86, 299.62 and 293.31 nm in ethanol solvent, respectively. On the other hand, it is well known that the highest occupied molecular orbital (HOMO) which implies the outermost orbital filled by electrons and behaves as an electron donor, but lowest unoccupied molecular orbital (LUMO) which can be considered as the first empty innermost orbital unfilled by electron and behaves as an electron acceptor are also called the frontier molecule orbitals (FMOs). The energy gap between HOMO and LUMO indicates the molecular chemical stability and is a critical parameter to determine molecular electrical transport properties [33]. In our study, HOMO – 1, HOMO, LUMO and LUMO + 1 energies and HOMOs–LUMOs energy gap values and their 3D plots of the compound **4** are shown in Fig 5.

4.4. Natural bond orbital (NBO) analysis

The natural bond orbital (NBO) analysis is used as an efficient tool to investigate the intra- and inter-molecular bondings as well as the charge transfers or conjugative interactions in molecular systems [34,35]. The NBO analysis is carried out by considering all possible interactions between the filled donor and empty acceptor natural bonds. In NBO analysis, the stabilization energy *E*(2) associated with electron delocalization between donor NBO (*i*) and acceptor NBO (*j*) is estimated using second-order perturbation theory and is given by,

$$E(2) = -q_i \frac{F_{ij}^2}{\Delta E} = -q_i \frac{\langle i|F|j \rangle^2}{\varepsilon_j - \varepsilon_i}$$

where *q_i* is the donor orbital occupancy, *ε_i* and *ε_j* are diagonal elements (orbital energies), and *F_{ij}* is the off-diagonal NBO Fock matrix element. The results of second-order perturbation theory analysis of the Fock Matrix at B3LYP/6-31G(d) level of theory are presented in Table S4 (Supplementary materials). Therefore we can easily state

that the highest energy values of hyperconjugative interactions in the title compound carried out the transitions between n electrons of N4 atom and π* of C5–O6 bonding (i.e. n_{N4} → π*_{C5–O6} and similarly n_{O19} → σ*_{O17–C18} and π_{N7–C8} → π*_{C9–C11} transition occur in title molecule.

4.5. Nonlinear optical (NLO) properties

The results of the calculated molecular polarizabilities at DFT/B3LYP/6-31G(d) level on the basis of the finite-field approach are given in Table 5. By considering Table 5, the values of the second-order polarizability or first hyperpolarizability β, dipole moment μ and polarizability α of title molecule are reported in the atomic mass units (a.u). In Gaussian03W output, the complete equations for calculating the magnitude of total static dipole moment μ_{total}, the mean polarizability α_{total}, the anisotropy of the polarizability Δα and the mean first hyperpolarizability β₀, by using the x, y, z components is defined as follows [36].

$$\alpha_{total} = \frac{1}{3}(\alpha_{xx} + \alpha_{yy} + \alpha_{zz})$$

$$\Delta\alpha = \frac{1}{\sqrt{2}}[(\alpha_{xx} - \alpha_{yy})^2 + (\alpha_{yy} - \alpha_{zz})^2 + (\alpha_{zz} - \alpha_{xx})^2 + 6\alpha_{xz}^2 + 6\alpha_{xy}^2 + 6\alpha_{yz}^2]^{\frac{1}{2}}$$

$$\beta_0 = [(\beta_{xxx} + \beta_{xyy} + \beta_{xzz})^2 + (\beta_{yyy} + \beta_{yzz} + \beta_{yxx})^2 + (\beta_{zzz} + \beta_{zxx} + \beta_{zyy})^2]^{\frac{1}{2}}$$

$$\mu_{total} = (\mu_x^2 + \mu_y^2 + \mu_z^2)^{\frac{1}{2}}$$

The polarizabilities and hyperpolarizability are reported in terms of atomic units (a.u) and the calculated values have been converted by using 1 a.u³ = (0.529)³ Å³ for α and 1 a.u = 8.641 × 10⁻³³ cm⁵/esu for β. In our calculations, the values of the calculated x, y, z components and total values of dipole moment was found to be 2.5670, 3.0572, 0.0717 and 3.9926 Debye, respectively. The calculated anisotropy of the polarizability of compound **4** is 27.838 Å³. The calculated first hyperpolarizability value (β) which is an important key factors for NLO properties of molecular system at the B3LYP/6-31G(d) level is equal to 10.617 × 10⁻³⁰ cm⁵/esu.

In NLO studies, the urea is used as reference and its calculated μ, α and β values at the B3LYP/6-31G(d) level were found as 1.3732 Debye, 3.8312 Å³ and 3.7289 × 10⁻³¹ cm⁵/esu, respectively [36]. Therefore the dipole moment, polarizability and first hyperpolarizability of title molecule are approximately 2.906, 7.266 and 28.470 times greater than those of urea.

4.6. Energies and dipole moments

The energetic behavior of title molecule was investigated in five solvents (vacuum (ε = 1.0000), chloroform (ε = 4.7113), ethanol (ε = 24.8520), DMSO (ε = 46.8260) and water (ε = 78.3553)). Total

Table 3

The experimental and calculated absorption wavelength (*λ*), excitation energies and oscillator strengths (*f*) of 1-acetyl-3-methyl-4-[3-methoxy-4-(4-methylbenzoxy)benzylidenedenamino]-4,5-dihydro-1*H*-1,2,4-triazol-5-one molecule (**4**).

Exp. (in ethanol) <i>λ</i> (nm)/ε (L mol ⁻¹ cm ⁻¹)	Transition	The calculated with B3LYP/6-31G(d) level in vacuum/ethanol solvents				
		Transition	Probability	<i>λ</i> _{max} (nm)	Excitation energy (eV)	<i>f</i> (oscillator strength)
310/16742	n → π*	H → L	0.66486	321.40/324.86	3.8576/3.8166	0.5314/0.5310
296/17906	π → π*	H → L	0.17755	298.05/299.62	4.1598/4.1380	0.1152/0.1294
		H → L+1	0.65601			
–	π → π*	H-1 → L	0.66795	292.49/293.31	4.2389/4.2270	0.0586/0.1770
242/26425	n → σ*	–	–	–	–	–

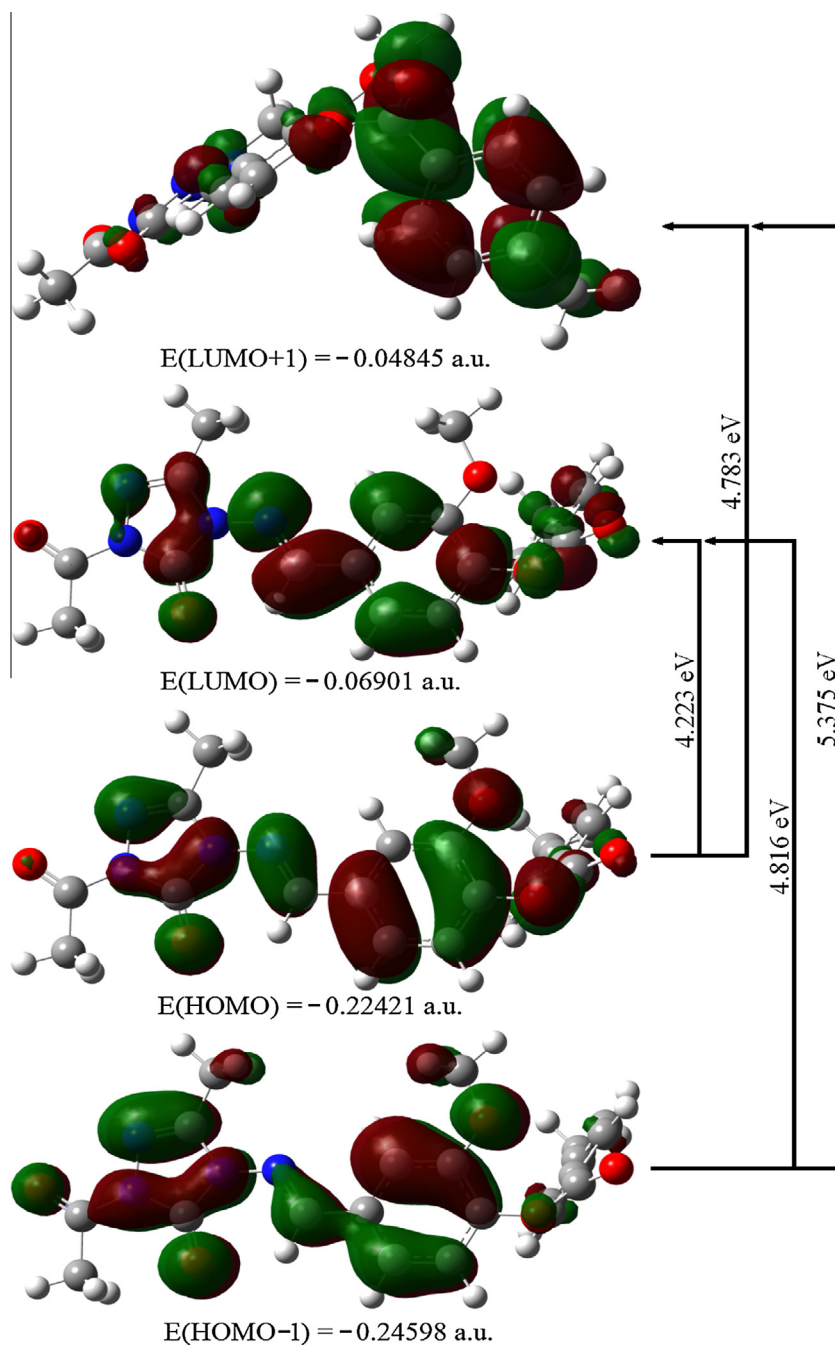


Fig. 5. 3D plots of HOMO – 1, HOMO, LUMO and LUMO + 1 of 1-acetyl-3-methyl-4-[3-methoxy-4-(4-methylbenzoxy)benzylideneamino]-4,5-dihydro-1H-1,2,4-triazol-5-one molecule (**4**) at the B3LYP/6-31G(d) level.

energy values and dipole moments in these solvents of title molecule were calculated by using B3LYP/6-31G(d) level with IEFPCM solvent model. The calculated energy values and dipole moment values are given in Table 6. As seen in Table 6, the calculated total molecular energy with IEFPCM solvent model of title molecule decreases with the increasing polarity of the solvent and the stability of the molecule increases. However, the calculated dipole moment by using IEFPCM solvent model for the title molecule increases with increasing polarity of the solvent.

4.7. Molecular electrostatic potential (MEP)

It is well-known that the molecular electrostatic potential (MEP) is useful for the understanding of the molecular interactions.

Furthermore, the MEP can be used for interpreting and predicting relative reactivities sites for electrophilic and nucleophilic attack, investigation of biological recognition, hydrogen bonding interactions, studies of zeolite, molecular cluster and crystal behavior and the correlation and prediction of a wide range of macroscopic properties [37]. The MEP is related to total charge distribution of the molecule and provides the correlations between the molecular properties such as partial charges, dipole moments, electronegativity and chemical reactivity.

The electrostatic potentials at the surface of title molecule are represented by different colors as seen in Fig. S6 (Supplementary materials). The negative electrostatic potential corresponds to a attraction of the proton by the concentrated electron density in the molecules, while positive electrostatic potential corresponds

Table 5

The electric dipol moment, polarizability and first order hyperpolarizability of 1-acetyl-3-methyl-4-[3-methoxy-4-(4-methylbenzoxy)benzylideneamino]-4,5-dihydro-1H-1,2,4-triazol-5-one molecule (**4**).

Parameters	Value (a.u)	Parameters	Value (a.u)
α_{xx}	399.0539316	β_{xxx}	-1313.4794429
α_{xy}	-21.5324957	β_{xyy}	202.8674630
α_{xz}	27.0607205	β_{xzz}	-78.6506096
α_{yy}	216.4382983	β_{yyy}	-273.0620136
α_{yz}	21.4309960	β_{yxx}	-80.9015819
α_{zz}	234.2426519	β_{yzz}	67.4959813
α_{total}	283.2449606	β_{zzz}	-84.2853153
$\Delta\alpha$	188.0951006	β_{xxx}	19.6294869
μ_x	2.5670	β_{yyz}	-50.2762441
μ_y	3.0572	β_0	1228.6653660
μ_z	0.0717		
μ_{total}	3.9926		

Table 6

Total energies and dipol moments in different solvents of 1-acetyl-3-methyl-4-[3-methoxy-4-(4-methylbenzoxy)benzylideneamino]-4,5-dihydro-1H-1,2,4-triazol-5-one molecule (**4**).

Solvent (ϵ ; dielectric constant)	Energy (Hartree)	Dipol moment (μ ; Debye)
Vacuum ($\epsilon = 1.0000$)	-1407.38565149	3.9926
Chloroform ($\epsilon = 4.7113$)	-1407.40017843	4.5605
Ethanol ($\epsilon = 24.8520$)	-1407.40560863	4.7914
DMSO ($\epsilon = 46.8260$)	-1407.40630290	4.8276
Water ($\epsilon = 78.3553$)	-1407.40662604	4.8473

to repulsion of the proton by the atomic nuclei in regions where low electron density exists and the nuclear charge is incompletely shielded. Therefore red color parts represent the regions of negative electrostatic potential while blue ones represent the regions of positive electrostatic potential. Furthermore the green color parts indicate the regions of zero potential. The negative regions of $V(r)$ potential are related to electrophilic reactivity, while the positive ones are related to nucleophilic reactivity. The MEP of the title molecule was calculated from optimized molecular structure at the B3LYP/6-31G(d) level and the 3D plot of MEP from two different points of view of the compound **4** are given in Fig. S6 (Supplementary materials). By considering Fig. S6 (Supplementary materials), the negative regions of MEP map are mainly localized on the N3, O6, O17, O19 and O50 atoms indicating the possible sites for electrophilic reactivity due to the electronegative property. The positive region of MEP map is localized on the hydrogen atoms indicating the possible sites for nucleophilic attack.

4.8. Atomic charges and thermodynamic properties

The Mulliken and NBO atomic charges and some thermodynamic parameters at the B3LYP/6-31 G(d) level of compound **4** in gas phase are given in Table S7 (Supplementary materials) [38].

The electronegative N1, N3, N4, O6, N7, O15, O17, O19 and O50 atoms of compounds **4** have negative atomic charge values. The atomic charges (Mulliken/NBO) of the mentioned atoms were calculated as -0.43089/-0.28434, -0.30707/-0.227178, -0.44730/-0.34133, -0.53483/-0.62902, -0.31881/-0.29286, -0.51833/-0.51792, -0.53114/-0.53384, -0.42875/-0.54161 vs -0.42159/-0.53420 a.u., respectively. The C2, C5, C8, C12, C14, C18 and C28 carbon atoms bounded to the mentioned electronegative atoms in the molecule under study have positive atomic charge values. The values of the positive charges of the mentioned carbon atoms were found as 0.55693/0.41865, 0.85903/0.78649, 0.03351/0.07493, 0.38736/0.28719, 0.31720/0.28364, 0.55260/

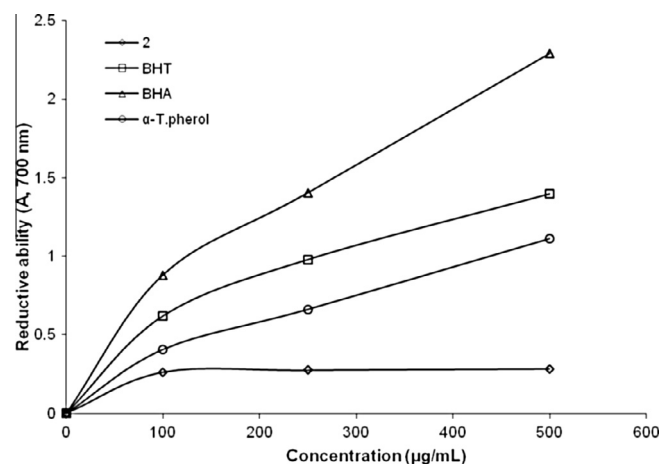


Fig. 7. Reducing power of different amount of compound **4**, BHT, BHA and α -tocopherol.

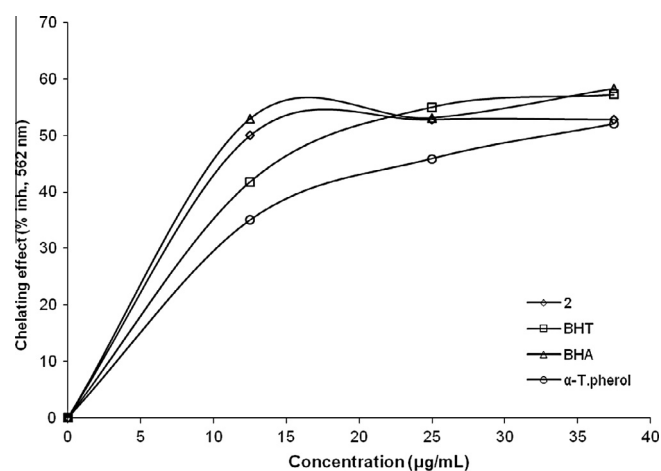


Fig. 8. Ferrous ion chelating activity of different amount of the compound **4**, BHT, BHA and α -tocopherol on ferrous ions.

0.83019 and 0.57305/0.71986 a.u., respectively. Therefore the C5 atom surrounded with the electronegative N1, N4 and O6 atoms and the C2 atom surrounded with two electronegative N1 and N3 atoms and the C18 atom surrounded with two electronegative O17 and O19 atoms have the highest positive charge values. Because the carbon atoms π bonding have more positive charge density compared to ones having only σ bonding. In other words, the charge density of the carbon atoms with sp^2 hybrids is greater than those of the carbon atoms with sp^3 hybrids. Therefore the title molecule shows strong delocalization energy. For example, the calculated Mulliken/NBO atomic charges of the C16, C26, C27 and C46 atoms which are in out of rings and are formed by sp^3 hybrids were found as -0.21782/-0.31507, -0.53164/-0.69142, -0.50855/-0.72366 vs -0.52172/-0.77354 a.u. In the compound **4** the atomic charges of all hydrogen atoms have positive values.

4.9. Antioxidant activity

The reductive capabilities of compounds were assessed by the extent of conversion of the Fe^{3+} /ferricyanide complex to the Fe^{2+} /ferrous form. The reducing power of the compound were observed at different concentrations, and results were compared with BHA, BHT and α -tocopherol (standard antioxidants). Fig. 7 shows the reducing activity of compound and standards. In the study, synthe-

sized compound **4** showed higher activities than blank. Reducing power of compound and standards were found as following order: BHA > BHT > α -tocopherol > compound **4**.

The hydrogen atoms or electrons donation ability of the synthesized compound and standard antioxidants such as BHA, BHT and α -tocopherol was measured by DPPH method. The reduction capability of DPPH radicals was determined by decrease in its absorbance at 517 nm induced by antioxidants. The obtained results indicate that the newly synthesized compound **4** did not show an effective activity as a radical scavenger, indicating that it has no activity as hydrogen donors.

Furthermore the ferrous ions chelating activities of synthesized compound **4**, BHA, BHT and α -tocopherol are shown in Fig. 8. The data obtained from our studies reveal that the synthesized compound demonstrates a marked capacity for iron binding, suggesting that their action as peroxidation protectors may be related to their iron binding capacity. The metal chelating effect of the compound and standards decreased in the order of BHA > BHT > compound **4** > α -tocopherol.

5. Conclusion

At the present work, the synthesis and *in vitro* antioxidant evaluation of 1-acetyl-3-methyl-4-[3-methoxy-4-(4-methylbenzoyloxy)benzylideneamino]-4,5-dihydro-1H-1,2,4-triazol-5-one molecule are defined. The studied compound demonstrates a marked capacity for iron binding. The data given here could be of the possible interest because of the observed metal chelating activities of the studied compounds could prevent redox cycling. The obtained results can be useful for the guidance of the development of novel triazole-based therapeutic target.

At the same time, the molecular structure, vibrational wavenumbers, the electronic absorption maximum wavelenghts, the HOMO, LUMO, MEP and NBO analyses, NLO properties, atomic charges and thermodynamic parameters of the synthesized 1-acetyl-3-methyl-4-[3-methoxy-4-(4-methylbenzoyloxy)benzylideneamino]-4,5-dihydro-1H-1,2,4-triazol-5-one molecule have been calculated at the B3LYP/6-31G(d) level of the theory for the first time. Furthermore it can be easily stated that the calculated vibrational frequencies and UV spectroscopic parameters are in a very good agreement with the experimental data.

Appendix A. Supplementary material

Supplementary data associated with this article can be found, in the online version, at <http://dx.doi.org/10.1016/j.molstruc.2013.10.044>.

References

- [1] H.H. Hussain, G. Babic, T. Durst, J.S. Wright, M. Fluerau, A. Chichirau, L.L. Chepelev, J. Org. Chem. 68 (2003) 7023–7032.
- [2] H. Yüksek, A. Demirbaş, A. İkizler, C.B. Johansson, C. Çelik, A.A. İkizler, Arzneimittel-Forsch. 47 (1997) 405–409.
- [3] Ö.G. Kol, H. Yüksek, E-J. Chem. 7 (2010) 123–136.
- [4] H. Bayrak, A. Demirbaş, S.A. Karaoğlu, N. Demirbaş, Eur. J. Med. Chem. 44 (2009) 1057–1066.
- [5] A.A. İkizler, F. Uçar, H. Yüksek, A. Aytin, I. Yasa, T. Gezer, Acta Pol. Pharm.-Drug Res. 54 (1997) 135–140.
- [6] M. Amir, M.S.Y. Khan, M.S. Zaman, Indian J. Chem. B 43 (2004) 2189–2194.
- [7] H. Yüksek, Ö.G. Kol, G. Kemer, Z. Ocak, B. Anil, Indian J. Heterocycl. Chem. 20 (2011) 325–330.
- [8] S. Bahçeci, H. Yüksek, Z. Ocak, I. Azakli, M. Alkan, M. Özdemir, Collect. Czech. Chem. C 67 (2002) 1215–1222.
- [9] H. Gökçe, S. Bahçeli, O. Akyıldırım, H. Yüksek, Ö.G. Kol, Lett. Org. Chem. 10 (2013) 395–441.
- [10] A.A. İkizler, H. Yüksek, Org. Prep. Proc. Int. 25 (1993) 99–105.
- [11] A.A. İkizler, R. Un, 7 (1979) 269–290; [Chem. Abstr. 1981, 94, 15645d].
- [12] M. Oyaizu, Japan Nutr. 44 (1986) 307–316.
- [13] M.S. Blois, Nature 181 (1958) 1199–1200.
- [14] P.D. Duh, Y.Y. Tu, G.C. Yen, Food Sci. Technol.-Leb. 32 (1999) 269–277.
- [15] T.C.P. Dinis, V.M.C. Madeira, L.M. Almeida, Arch. Biochem. Biophys. 315 (1994) 161–169.
- [16] F. Yamaguchi, T. Ariga, Y. Yoshimura, H. Nakazawa, J. Agric. Food Chem. 48 (2000) 180–185.
- [17] M.J. Frisch, G.W. Trucks, H.B. Schlegel, G.E. Scuseria, M.A. Robb, J.R. Cheeseman, J.A. Montgomery Jr., T. Vreven, K.N. Kudin, J.C. Burant, J.M. Millam, S.S. Iyengar, J. Tomasi, V. Barone, B. Mennucci, M. Cossi, G. Scalmani, N. Rega, G.A. Petersson, H. Nakatsuji, M. Hada, M. Ehara, K. Toyota, R. Fukuda, J. Hasegawa, M. Ishida, T. Nakajima, Y. Honda, O. Kitao, H. Nakai, M. Klene, X. Li, J.E. Knox, H.P. Hratchian, J.B. Cross, C. Adamo, J. Jaramillo, R. Gomperts, R.E. Stratmann, O. Yazyev, A.J. Austin, R. Cammi, C. Pomelli, J.W. Ochterski, P.Y. Ayala, K. Morokuma, G.A. Voth, P. Salvador, J.J. Dannenberg, V.G. Zakrzewski, S. Dapprich, A.D. Daniels, M.C. Strain, O. Farkas, D.K. Malick, A.D. Rabuck, K. Raghavachari, J.B. Foresman, J.V. Ortiz, Q. Cui, A.G. Baboul, S. Clifford, J. Cioslowski, B.B. Stefanov, G. Liu, A. Liashenko, P. Piskorz, I. Komaromi, R.L. Martin, D.J. Fox, T. Keith, M.A. Al-Laham, C.Y. Peng, A. Nanayakkara, M. Challacombe, P.M.W. Gill, B. Johnson, W. Chen, M.W. Wong, C. Gonzalez, J.A. Pople, Gaussian 03, Revision D.01, Gaussian Inc., Wallingford, CT, 2004.
- [18] A. Frisch, A.B. Nielson, A.J. Holder, GAUSSVIEW User Manual, Gaussian, Inc., Wallingford, CT, 2003.
- [19] A.D. Becke, J. Chem. Phys. 98 (1993) 5648.
- [20] C. Lee, W. Yang, R.G. Parr, Phys. Rev. B 37 (1988) 785.
- [21] J.B. Foresman, E. Frisch, Exploring Chemistry with Electronic Structure Methods, Gaussian Inc., Pittsburgh, PA, USA, 1993.
- [22] A.P. Scott, L. Radom, J. Phys. Chem. 100 (1996) 16502–16513.
- [23] M.H. Jamroz, Vibrational Energy Distribution Analysis VEDA4, Warsaw, 2004.
- [24] A. Vlcek Jr., S. Zalis, Coord. Chem. Rev. 251 (2007) 258–287.
- [25] G. Keresztury, S. Holly, J. Varga, G. Besenyei, A.Y. Wang, J.R. Durig, Spectrochim. Acta A49 (1993) 2007.
- [26] G. Keresztury, in: J.M. Chalmers, P.R. Griffith (Eds.), Raman Spectroscopy: Theory in Hand book of Vibrational Spectroscopy, vol. 1, John Wiley & Sons Ltd., New York, 2002.
- [27] B.H. Stuart, Infrared Spectroscopy: Fundamentals and Applications, John Wiley & Sons, England, 2004.
- [28] R.M. Silverstein, F.X. Webster, Spectroscopic Identification of Organic Compound, sixth ed., John Wiley & Sons, New York, 1998.
- [29] G. Varsanyi, Vibrational Spectra of Benzene Derivatives, Academic Press, New York, 1969.
- [30] D.L. Pavia, G.M. Lampman, G.S. Kriz, J.R. Vyvyan, Introduction to Spectroscopy, Brooks/Cole Cengage Learning, USA, 2009.
- [31] L.J. Bellamy, The Infrared Spectra of Complex Molecules, third ed., Wiley, New York, 1975.
- [32] N.B. Colthup, L.H. Daly, E. Wiberley, Introduction to Infrared and Raman Spectroscopy, Academic Press, New York, 1964.
- [33] K. Fukui, Science 218 (1982) 747.
- [34] F. Wienhold, C.R. Landis, Valency and Bonding – A Natural Bond Orbital-Acceptor Perspective, Cambridge University Press, New York, 2005.
- [35] F.L. Huyskens, P.L. Huyskens, A.P. Pearson, J. Chem. Phys. 108 (1998) 8161.
- [36] Y.-X. Sun, Q.-L. Hao, Z.-X. Yu, W.-X. Wei, L.-D. Lu, X. Wang, Mol. Phys. 107 (2009) 223–235.
- [37] J.S. Murray, K. Sen, Molecular Electrostatic Potentials Concepts and Applications, Elsevier Science B.V., Amsterdam, The Netherlands, 1996.
- [38] R.S. Mulliken, J. Chem Phys. 23 (1955) 1833–1840.